Nonlocal kinetic energy functional from the jellium-with-gap model: Applications to orbital-free density functional theory

Lucian A. Constantin,[1] Eduardo Fabiano,[1,2] and Fabio Della Sala[1,2]

[1]*Center for Biomolecular Nanotechnologies @UNILE, Istituto Italiano di Tecnologia, Via Barsanti, I-73010 Arnesano, Italy*
[2]*Institute for Microelectronics and Microsystems (CNR-IMM), Via Monteroni, Campus Unisalento, 73100 Lecce, Italy*

Orbital-free density functional theory (OF-DFT) promises to describe the electronic structure of very large quantum systems, being its computational cost linear with the system size. However, the OF-DFT accuracy strongly depends on the approximation made for the kinetic energy (KE) functional. To date, the most accurate KE functionals are nonlocal functionals based on the linear-response kernel of the homogeneous electron gas, i.e., the jellium model. Here, we use the linear-response kernel of the jellium-with-gap model to construct a simple nonlocal KE functional (named KGAP) which depends on the band-gap energy. In the limit of vanishing energy gap (i.e., in the case of metals), the KGAP is equivalent to the Smargiassi-Madden (SM) functional, which is accurate for metals. For a series of semiconductors (with different energy gaps), the KGAP performs much better than SM, and results are close to the state-of-the-art functionals with sophisticated density-dependent kernels.

I. INTRODUCTION

The main quantity in the density functional theory (DFT) [1,2] is the ground-state electron density $n(\mathbf{r})$. In the most straightforward realization of DFT, i.e., orbital-free (OF) DFT, the electron density is found by solving the Euler equation [2]

$$\frac{\delta T_s[n]}{\delta n(\mathbf{r})} + v_{\text{ext}}(\mathbf{r}) + \int d\mathbf{r}' \frac{n(\mathbf{r}')}{|\mathbf{r} - \mathbf{r}'|} + \frac{\delta E_{\text{XC}}[n]}{\delta n(\mathbf{r})} = \mu, \quad (1)$$

where $T_s[n]$ is the noninteracting kinetic energy (KE) functional, $v_{\text{ext}}(\mathbf{r})$ is the external potential, $E_{\text{XC}}[n]$ is the exchange-correlation (XC) energy functional, and μ is a Lagrange multiplier fixed from the normalization condition $\int d\mathbf{r}\, n(\mathbf{r}) = N$, with N being the total number of electrons. Both $T_s[n]$ and $E_{\text{XC}}[n]$ are unknown and they must be approximated. Many valuable approximations, even at the semilocal level of theory, have been developed for E_{XC} [3,4]. On the other hand, accurate approximations of $T_s[n]$ are much harder to obtain [5–8] because this term usually gives the dominant contribution to the ground-state energy [2] and especially because of its highly nonlocal nature [5,7,9–12].

This problem is bypassed in the Kohn-Sham (KS) [13] formalism where the noninteracting KE is treated exactly via the one-particle orbitals of an auxiliary system of non-interacting particles. In this way, practical DFT calculations in both quantum chemistry and material science are made routinely possible [14,15]. However, one has to pay the cost of the introduction of orbitals into the formalism, which makes the method formally scale as $O(N^3)$. To overcome this limit, various fast electronic structure approaches have been developed, such as linear scaling $O(N)$ methods based on density matrix approximations [16,17], as well as tight-binding and semiempirical methods [18–20]. Anyway, these methods are numerically quite cumbersome if compared to the elegant OF-DFT approach. Thus, intensive investigations are performed in the field of KE functional approximations

suitable to OF-DFT [5,6], and important OF-DFT large-scale applications have been studied [21–29].

Kinetic energy functionals can be written in the general form

$$T_s[n] = \int \tau[n](\mathbf{r}) d\mathbf{r}, \quad (2)$$

where τ is the KE density, which is formally defined as $\tau(\mathbf{r}) = \sum_i |\nabla\phi_i(\mathbf{r})|^2/2$, with $\phi_i(\mathbf{r})$ being the ith occupied Kohn-Sham orbital. For other (equivalent) formal definitions of τ, see for example Refs. [30,31].

Approximations of $\tau(\mathbf{r})$ can be classified on a ladder of complexity. The first rung contains functionals whose KE density is only a function of the density $\tau(\mathbf{r}) = \tau(n(\mathbf{r}))$, such as Thomas-Fermi (TF) [32,33]. The TF theory [32–34] can not bind atoms into molecules [35], although it is asymptotically correct for heavy atoms and molecules [36–40] and accounts for the stability of bulk matter [36]. Nevertheless, for the simple extension of the TF theory with the von Weizsäcker kinetic energy [41], Lieb *et al.* have mathematically proven the existence of binding for two very dissimilar atoms [42]. This fact encouraged the investigation of exact KE properties [30,31,43–51], and the development of semilocal KE functional approximations. The simplest of them are found on the second rung of the ladder and are mainly represented by the generalized gradient approximations (GGAs), of the form $\tau^{\text{GGA}}(\mathbf{r}) = \tau(n(\mathbf{r}), \nabla n(\mathbf{r}))$. Starting with von Weizsäcker [41] and second-order gradient expansion [52], there are many GGA functionals constructed from exact conditions [53–57], model systems [58–61], and empirical considerations [62–65]. Often these semilocal functionals display several drawbacks and have limited applicability in the context OF-DFT calculations [66]. However, some notable exceptions also exist [6,66–72]. Among them we mention the VT84F GGA of Ref. [72], and the vWGTF1 and vWGTF2 of Ref. [66], that can be considered state-of-the-art semilocal functionals for OF-DFT [6,66,68,69]. On the third rung of the ladder

are the Laplacian-level meta-GGA functionals, with the form $\tau^{\mathrm{MGGA}}(\mathbf{r}) = \tau(n(\mathbf{r}), \nabla n(\mathbf{r}), \nabla^2 n(\mathbf{r}))$. The most known meta-GGA is the fourth-order gradient expansion of the uniform electron gas [73,74], that had been applied to metallic clusters in the OF-DFT context [75,76]. Several meta-GGAs have been recently developed [77–80] for various purposes, including OF-DFT for solids [80]. The next rung includes the class of u-meta-GGA functionals. Such approximations have been recently proposed [81,82] and they use as additional ingredient the Hartree potential $u(\mathbf{r}) = \int d\mathbf{r}' n(\mathbf{r}')/|\mathbf{r} - \mathbf{r}'|$, such that the KE density has the form

$$\tau^{u\mathrm{MGGA}}(\mathbf{r}) = \tau(n(\mathbf{r}), \nabla n(\mathbf{r}), \nabla^2 n(\mathbf{r}), u(\mathbf{r})). \quad (3)$$

The u-meta-GGAs are promising tools for OF-DFT, but they require further investigations before they can become practical tools for these calculations.

Up to this level, the ladder of KE functionals contains only semilocal approximations, i.e., functions that use as input ingredients only the electron density at a given point in the space and other quantities (typically spatial derivatives of the density) computed at the same point. These approximations are computationally very advantageous because of their local nature, and are theoretically justified by the the concept of nearsightedness of electrons, which means that the density $n(\mathbf{r})$ depends significantly only on the effective external potential at nearby points [83]. Consequently, any local physical property at point $\mathbf{r}$ can be described by the density behavior in a small volume dV around this point. However, this principle does not hold in general and, especially for KE [12,84], the nonlocal effects can not be ruled out in all cases. The consequence is that semilocal KE functionals face several limitations. In fact, in view of overcoming this problem, the u-meta-GGA already contains important nonlocality through the Hartree-potential ingredient. The fundamental solution, anyway, is to consider fully nonlocal KE approximations.

Nowadays, the most sophisticated KE functionals are the fully nonlocal ones [85–96]. Most of them can be written in the generic form

$$T_s[n] = T_s^{\mathrm{TF}} + T_s^W + \langle n(\mathbf{r})^\alpha | w(\mathbf{r} - \mathbf{r}', n(\mathbf{r}), n(\mathbf{r}')) | n(\mathbf{r}')^\beta \rangle, \quad (4)$$

where $T_s^{\mathrm{TF}} = \frac{3}{10}(3\pi^2)^{2/3} \langle n(\mathbf{r})^{5/3} \rangle$, and $T_s^W = \langle \frac{|\nabla n(\mathbf{r})|^2}{8n(\mathbf{r})} \rangle$ are the TF and von Weizsäcker functionals, respectively, α and β are parameters, and the kernel $w(\mathbf{r} - \mathbf{r}', n(\mathbf{r}), n(\mathbf{r}'))$ is chosen such that $T_s[n]$ recovers the exact linear response (LR) of the noninteracting uniform electron gas without exchange [85,86,97]:

$$\hat{\mathcal{F}}\left(\frac{\delta^2 T_s[n]}{\delta n(\mathbf{r})\delta n(\mathbf{r}')}\Big|_{n_0}\right) = -\frac{1}{\chi_{\mathrm{Lind}}} = \frac{\pi^2}{k_F} F^{\mathrm{Lind}}(\eta), \quad (5)$$

with

$$F^{\mathrm{Lind}} = \left(\frac{1}{2} + \frac{1 - \eta^2}{4\eta} \ln\left|\frac{1 + \eta}{1 - \eta}\right|\right)^{-1} \quad (6)$$

being the Lindhard function [5,98], $\eta = q/(2k_F)$ being the dimensionless momentum [q is the momentum and $k_F = (3\pi^2 n_0)^{1/3}$ is the Fermi wave vector of the jellium with the constant density n_0], and $\hat{\mathcal{F}}(\cdot)$ denotes the Fourier transform. The most simple functionals having the form of Eq. (4) are the

ones with a density-independent kernel $w(\mathbf{r} - \mathbf{r}')$, which are also the most attractive from the computational point of view. After using the constraint of Eq. (5), they depend only on the choice of the parameters α and β. The most known functionals of this class are as follows:

(i) the Perrot functional [99], with $\alpha = \beta = 1$;

(ii) the Wang-Teter (WT) functional [100], with $\alpha = \beta = \frac{5}{6}$;

(iii) the Smargiassi and Madden (SM) functional [101], with $\alpha = \beta = \frac{1}{2}$;

(iv) the Wang-Govind-Carter (WGC) functional [97], with $\alpha, \beta = \frac{5}{6} \pm \frac{\sqrt{5}}{6}$.

In the context of orbital-free DFT, these KE functionals are usually accurate for structural properties of simple metals [97], systems for which the LR of jellium is an excellent model. However, they may fail for other bulk solids, such as semiconductors and insulators, where the jellium perturbed by a small-amplitude, short-wavelength density wave is not a relevant model.

To improve the description of semiconductors, the Huang-Carter (HC) functional has been introduced [85]. The kernel of this functional is more complicated, being dependent on the density and the gradient of the density, as well as on empirical parameters. This functional, as any nonlocal KE functional [97], has a quasilinear scaling with system size (N), behaving as $O(N \ln(N))$, but its prefactor may be quite large [87], lowering considerably the overall computational efficiency. Consequently, it is significantly slower than nonlocal KE functionals with density-independent kernels.

Computationally efficient methods/functionals for semiconductors have been recently developed. Thus, the density-decomposed WGCD KE functional [102], as well as the enhanced von Weizsäcker–WGC (EvW-WGC) KE functional [87] are both based on the WGC density-dependent kernel [97]. These functionals, which also contain several empirical parameters, are a hundred times faster than HC, providing similar accuracy as the HC functional, for semiconductors. Additionally, the EvW-WGC functional accurately describes metal-insulator transitions [87,103]. However, we mention that, in contrast to HC, the WGCD and EvW-WGC can not be written in the form of Eq. (4).

In this paper, we introduce a nonlocal KE functional with a density-independent kernel (KGAP) that recovers not Eq. (5) but the LR of the jellium-with-gap model [61,104]. This is an important generalization of the uniform electron gas, that has already been used to have qualitative and quantitative insight for semiconductors [104–108], to develop an XC kernel for the optical properties of materials [109], and to construct accurate functionals for the ground-state DFT [110–115]. Recently, the KE gradient expansion of the jellium with gap has also been derived and used in the construction of semilocal KE functionals [61]. The KGAP functional fulfills important exact properties and shows a better accuracy as well as a broader applicability than other existing nonlocal functionals with a density-independent kernel.

The paper is organized as follows. In Sec. II, we construct the KGAP functional, and in Sec. IV we test it for equilibrium lattice constants and bulk moduli of several bulk solids, performing full OF-DFT calculations. Computational details of these calculations are presented in Sec. III. Finally, in Sec. V we summarize our results.

II. THEORY

Let us consider a generalization of Eq. (4) of the form

$$T_s[n] = \lambda T_s^{\mathrm{TF}} + \mu T_s^W + \langle n(\mathbf{r})^\alpha | w(\mathbf{r} - \mathbf{r}', E_g) | n(\mathbf{r}')^\beta \rangle, \quad (7)$$

where $\lambda, \mu \in [0,1]$ as well as α and β are positive parameters, and $w(\mathbf{r} - \mathbf{r}', E_g)$ is a density-independent kernel chosen such that the whole KE functional $T_s[n]$ satisfies the LR of the jellium-with-gap model [61,104]

$$\hat{\mathcal{F}}\left(\frac{\delta^2 T_s[n]}{\delta n(\mathbf{r}) \delta n(\mathbf{r}')}\bigg|_{n_0}\right) = -\frac{1}{\chi_{\mathrm{GAP}}} = \frac{\pi^2}{k_F} F^{\mathrm{GAP}}(\eta), \quad (8)$$

with

$$1/F^{\mathrm{GAP}} = \frac{1}{2} - \frac{\Delta\left[\arctan\left(\frac{4\eta + 4\eta^2}{\Delta}\right) + \arctan\left(\frac{4\eta - 4\eta^2}{\Delta}\right)\right]}{8\eta}$$
$$+ \left(\frac{\Delta^2}{128\eta^3} + \frac{1}{8\eta} - \frac{\eta}{8}\right) \ln\left(\frac{\Delta^2 + (4\eta + 4\eta^2)^2}{\Delta^2 + (4\eta - 4\eta^2)^2}\right), \quad (9)$$

where $\Delta = 2E_g/k_F^2$, with E_g being the gap. In momentum space, the kernel w is

$$w(\mathbf{q}) = -\frac{\chi_{\mathrm{GAP}}^{-1} - \lambda \chi_{\mathrm{TF}}^{-1} - \mu \chi_W^{-1}}{2\alpha\beta n_0^{\alpha+\beta-2}}$$
$$= \frac{5}{9\alpha\beta n_0^{\alpha+\beta-5/3}}[F^{\mathrm{GAP}}(\eta) - \lambda - 3\mu\eta^2], \quad (10)$$

with $\chi_{\mathrm{TF}} = -k_F/\pi^2$, and $\chi_W = -k_F/(3\pi^2\eta^2)$. Some details on the derivation of Eq. (10) are given in Appendix A.

A careful analysis of F^{GAP} is provided in Ref. [61]. The most important features of F^{GAP} are also summarized in the Appendix B. Here, we use them, together with the procedure proposed in Refs. [86,97], to find the low-q (at $\Delta \to 0$) and high-q (at any Δ) limits of the functional of Eq. (7). Some details of the derivation of these limits are given in Appendix C. The mentioned limits are

$$\lim_{\mathbf{q}\to 0} T_s[n] \to \left[\lambda + \frac{5}{9\alpha\beta}(1-\lambda)\right]T_s^{\mathrm{TF}} + \frac{T_s^W}{9} + \frac{5(1-\lambda)}{9\alpha\beta}\left(\alpha + \beta - \frac{5}{3}\right)\left\{\langle\delta n|\tau_{\mathrm{TF}}\rangle + \left(\alpha+\beta-\frac{8}{3}\right)\frac{\langle\delta^2 n|\tau_{\mathrm{TF}}\rangle}{2}\right\}$$
$$+ \left(\frac{1}{9} - \mu\right)(\alpha+\beta-1)\left\{\langle\delta n|\tau_W\rangle + (\alpha+\beta-2)\frac{\langle\delta^2 n|\tau_W\rangle}{2}\right\} + O(\delta^3 n), \quad (11)$$

$$\lim_{\mathbf{q}\to\infty} T_s[n] \to T_s^W + \left(\lambda - \frac{1}{3\alpha\beta} - \frac{5\lambda}{9\alpha\beta}\right)T_s^{\mathrm{TF}} - \frac{3+5\lambda}{9\alpha\beta}\left(\alpha+\beta-\frac{5}{3}\right)\left\{\langle\delta n|\tau_{\mathrm{TF}}\rangle + \left(\alpha+\beta-\frac{8}{3}\right)\frac{\langle\delta^2 n|\tau_{\mathrm{TF}}\rangle}{2}\right\}$$
$$+ (1-\mu)(\alpha+\beta-1)\left\{\langle\delta n|\tau_W\rangle + (\alpha+\beta-2)\frac{\langle\delta^2 n|\tau_W\rangle}{2}\right\} + O(\delta^3 n), \quad (12)$$

where $\delta n = n(\mathbf{r})/n_0 - 1$. Equation (11) is a generalization of Eq. (17) of Ref. [97], recovering it for the case $\lambda = \mu = 1$. In this low-q limit the exact behavior is described by the second-order gradient expansion (GE2) (i.e., $T_s^{\mathrm{GE2}} = T_s^{\mathrm{TF}} + T_s^W/9$). This is recovered whenever

$$\lambda = 1 \quad \text{and} \quad \left(\frac{1}{9} - \mu\right)(\alpha+\beta-1) = 0 \quad (13)$$

or independently on the values of α and β, when $\lambda = 1$ and $\mu = \frac{1}{9}$. The only functional with the form of Eq. (7) that is correct in the limit $\mathbf{q} \to 0$ is the SM functional ($\alpha = \beta = \frac{1}{2}$, $\lambda = 1$, $\mu = 1$, and $E_g = 0$). Note, anyway, that for $\mathbf{q} \to 0$ we have $T_s^{\mathrm{TF}} \gg T_s^W$, thus, any functional recovering correctly the TF behavior is accurate.

For the case $\mathbf{q} \to \infty$, F^{GAP} behaves as F^{Lind} for any Δ, and we recover Eq. (18) of Ref. [97] when $\lambda = \mu = 1$. The exact LR behavior [61] is

$$\lim_{\mathbf{q}\to\infty} T_s[n] \to T_s^W - \frac{3}{5}T_s^{\mathrm{TF}}, \quad (14)$$

which can be satisfied if

$$\lambda - \frac{3+5\lambda}{9\alpha\beta} = -\frac{3}{5},$$
$$\left(\alpha+\beta-\frac{5}{3}\right)\frac{3+5\lambda}{9\alpha\beta} = 0,$$

$$(1-\mu)(\alpha+\beta-1) = 0. \quad (15)$$

Only the WGC functional ($\alpha, \beta = \frac{5}{6} \pm \frac{\sqrt{5}}{6}$, $\lambda = \mu = 1$, $E_g = 0$) is correct in the limit $\mathbf{q} \to \infty$. We also remark that, in this limit, $T_s^W \gg T_s^{\mathrm{TF}}$, therefore, in principle, any functional with the form of Eq. (7) and with $\mu = 1$ does not fail badly in this limit.

Inspection of Eqs. (13) and (15) shows that it is not possible to fix the parameters in order to satisfy exactly both the low- and high-q limits. Nevertheless, the choice

$$\lambda = 1, \quad \mu = 1 \quad (16)$$

allows to recover in both cases the correct leading term, guaranteeing that $T_s[n]$ performs reasonably well in both limits, independently on α and β ($\alpha, \beta > 0$). This choice appears then to be the most physical for a kinetic functional. Moreover, in the low-q limit the correct behavior is anyway obtained fixing $\alpha = \alpha^{LQ} = \frac{1}{2}$ and $\beta = \beta^{LQ} = \frac{1}{2}$; similarly, in the high-q limit this occurs for $\alpha = \alpha^{HQ} = \frac{5}{6} + \frac{\sqrt{5}}{6}$ and $\beta = \beta^{HQ} = \frac{5}{6} - \frac{\sqrt{5}}{6}$.

We can use these observations to propose a kinetic functional based on Eq. (7). This is named KGAP and uses $\lambda = 1$ and $\mu = 1$ as well as

$$\alpha^{\mathrm{KGAP}} = \alpha^{LQ} + (\alpha^{HQ} - \alpha^{LQ})\frac{E_g^2}{b + E_g^2}, \quad (17)$$

$$\beta^{\mathrm{KGAP}} = \beta^{LQ} + (\beta^{HQ} - \beta^{LQ})\frac{E_g^2}{b + E_g^2}, \qquad (18)$$

where $b = 5$ eV^2 is a parameter that controls the connection between the low- and high-q limits. Overall, the KGAP functional satisfies the following conditions: (1) for metals ($E_g = 0$), $F^{\mathrm{GAP}} = F^{\mathrm{Lind}}$ and KGAP performs as the SM functional, recovering GE2 for slowly varying densities; (2) for semiconductors and insulators, KGAP is correct at $\mathbf{q} \to 0$ [see Eqs. (B1) and (B2)]. This important exact condition is very difficult to be fulfilled, and even the HC functional constructed for semiconductors can not satisfy it [85]; (3) for large-gap insulators, KGAP correctly recovers the exact behavior of Eq. (14).

III. COMPUTATIONAL DETAILS

The KGAP functional has been implemented in PROFESS 3.0 (Princeton orbital-free electronic structure software), a plane-wave-based OF-DFT code [116]. We have then tested it for the simulation of cubic-diamond Si, various III-V cubic zinc-blende semiconductors (AlP, AlAs, AlSb, GaP, GaAs, GaSb, InP, InAs, and InAs) [87], and several metals, namely, Al, Mg, and Li, in their simple-cubic (sc), face-centered-cubic (fcc), and body-centered-cubic (bcc) structures. The results have been compared to those obtained with the SM and HC functionals. In this work, we use the HC with optimized parameters for semiconductors [85] ($\lambda = 0.01177$, and $\beta = 0.7143$). On the other hand, using the Perrot, WT, or WGC functionals almost no well-converged result could be obtained for the tested semiconductors.

For a better comparison with literature results, we have used the Perdew and Zunger XC LDA parametrization [117] for semiconductors and the Perdew–Burke–Ernzerhof (PBE) [118] XC functional for metals, bulk-derived local pseudopotentials (BLPSs), as in Refs. [66,87], and plane-wave basis kinetic energy cutoffs of 1600 eV. Equilibrium volumes and bulk moduli have been calculated by expanding and compressing the optimized lattice parameters by up to about 10% to obtain 30 energy-volume points and then fitting with the Murnaghans equation of state [119].

IV. RESULTS

A. Energy gap

The KGAP functional, defined by Eqs. (7), (10), and (16)–(18), depends on the energy gap E_g. Previous investigation on exchange-correlation kernel indicated that E_g can be fixed to the experimental fundamental gap of semiconductors and insulators [109]. In this section we will verify if this can be considered a good approximation also for the kinetic energy.

In Fig. 1, we report the errors on equilibrium volumes (Å^3/cell) and bulk moduli (GPa) for AlAs and GaSb, as a function of the parameter E_g. We recall that setting $E_g = 0$, the KGAP functional is equivalent to the SM functional, which is not accurate for semiconductors, as shown in Fig. 1. When E_g is increased, the errors decrease for both systems and properties vanishing near the the vertical lines, which indicate the experimental fundamental gaps of AlAs (2.23 eV)
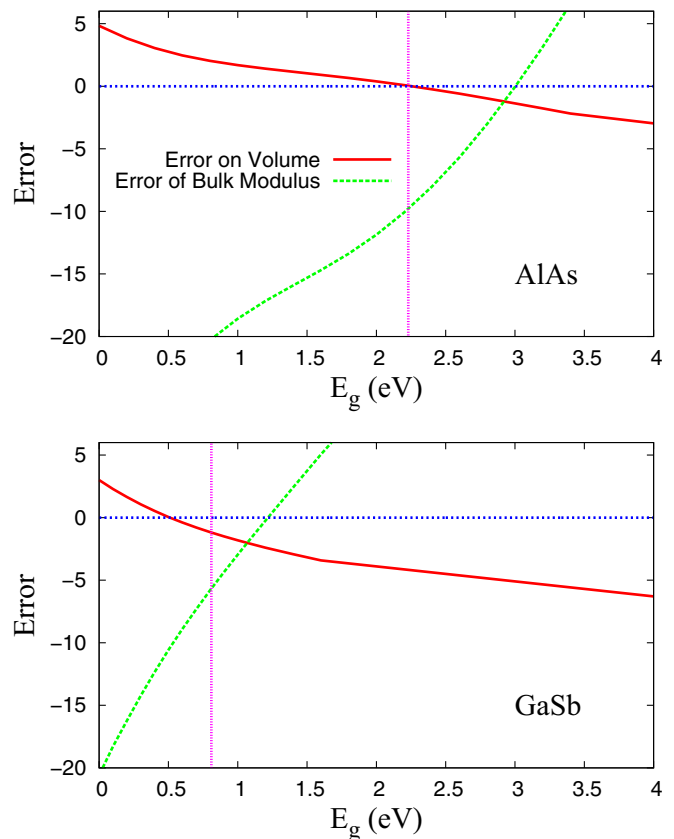

FIG. 1. Errors of KGAP OF-DFT calculations with respect to the KS-DFT references (OFDFT-KSDFT) for equilibrium volumes (Å^3/cell, red lines), and for bulk modulus (GPa, green lines), as a function of the energy-gap parameter E_g (in eV), for the AlAs and GaSb semiconductors. The experimental fundamental band gaps are shown with horizontal lines ($E_g = 2.23$ eV and 0.81 eV for AlAs and GaSb, respectively).

and GaSb (0.81 eV). Similar results are obtained for other semiconductors.

Next, in Fig. 2, we show the OF-DFT densities of Si and GaAs along the [111] direction, computed with several KE functionals. In both panels, all functionals, with the exception of the $E_g = 10$ eV extreme case, agree well in most of the space and more significant differences are obtained only at the bonding region, in the range between 0.4 and 0.8. Here, the SM functional (i.e., the KGAP with $E_g = 0$) gives smaller densities than the HC ones, with pronounced oscillatory features. On the other hand, the KGAP functional with the exact experimental band gap gives accurate densities, being of comparable accuracy as the HC ones. We also note that the results obtained from KGAP with $E_g = 10$ eV are inaccurate because of an unrealistic value of the E_g parameter. Nevertheless, even in this extreme case, the densities are smooth and the calculations are numerically stable. These facts are strong indications that F^{GAP} is a useful, well-behaved generalization of F^{Lind}.

The results of Figs. 1 and 2 show that the experimental fundamental gap is a good choice for the E_g parameter of the KGAP functional. Hence, unless differently stated, in all our calculations we fixed E_g to the experimental fundamental gap value of the investigated material. Finally, we mention
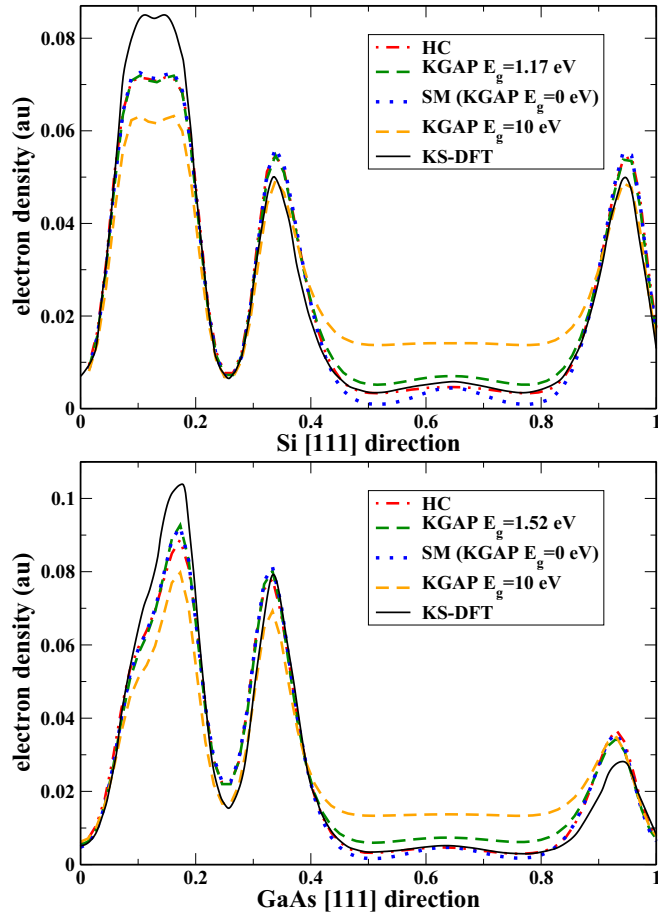
FIG. 2. Electron densities of Si (upper panel) and GaAs (lower panel) along the [111] direction, obtained from OF-DFT calculations with several KE functionals. The results for KGAP use the exact experimental band gaps ($E_g = 1.17$ eV for Si and 1.52 eV for GaAs, respectively), the vanishing band-gap case ($E_g = 0$) which represents the SM functional, and the case $E_g = 10$ eV. For comparison, see also Figs. 8 and 9 of Ref. [87].

that, due to its E_g dependence, the KGAP can be considered a semiempirical functional.

B. Global assessment for semiconductors and metals

In Fig. 3 we show the total energy versus volume curves for GaSb, GaAs, and GaP bulk solids, computed using various KE functionals. We observe that for all three cases, the Perrot, WT, and WGC functionals do not predict any binding. Moreover, their failures are accentuated when the fundamental band gap of the material E_g increases. For example, the Perrot functional gives converged results for GaSb ($E_b = 0.81$ eV), while it converges only within few points in the cases of GaAs ($E_b = 1.52$ eV) and GaP ($E_b = 2.35$ eV). Also, the quality of the WT and WGC results diminishes for GaAs and GaP in comparison with GaSb. On the other hand, SM always yields a bound result, but the potential energy curves are generally rather flat and the minima are always moved towards too large volumes. Finally, KGAP can consistently reproduce the reference values with good accuracy. Nevertheless, inspection of the figures shows that the KGAP functional yields a quite
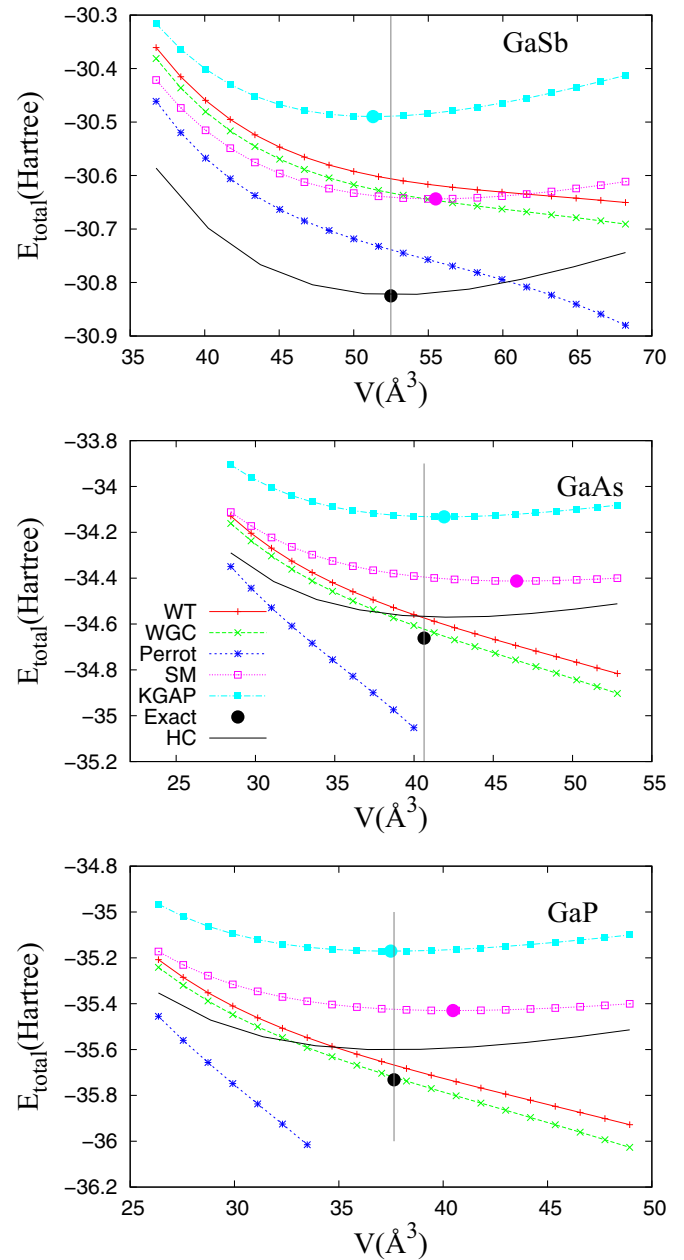

FIG. 3. Total energy (in Hartree) versus the volume of the unit cell (in Å^3) computed using OF-DFT calculations with several nonlocal functionals with density-independent kernels (Perrot [99], WT [100], WGC [97], SM [101], and KGAP) for GaSb (upper panel), GaAs (middle panel), and GaP (lower panel). The KS-DFT equilibrium point (denoted as Exact) is shown with black big dot. The SM and KGAP equilibrium points are also emphasized with big dots. For comparison, we also show the results of the HC [85] state-of-the-art nonlocal KE functional with a density-dependent kernel.

systematic overestimation of the total energies, giving a shift about 0.5 Hartree towards higher energies. Such a behavior is explained by Eq. (B6). This feature is anyway not a serious flaw for the functional since absolute energies are rarely important, whereas relative energies (such as in potential energy curves) are well described by KGAP.

TABLE I. Errors of OF-DFT with respect to the KS-DFT references (OFDFT–KSDFT) for equilibrium volumes ($\mathring{A}^3$/cell), computed from different KE functionals. The KS reference values (from Refs. [66,87]) are reported in the last column, and the exact band-gap energies (in eV) used for the KGAP functional are shown in the second column. The last lines of every panel report the mean absolute errors (MAE).

	E_g (eV)	SM	KGAP	HC	KS
Semiconductors					
Si	1.17	1.3	−0.3	0.0	19.781
GaP	2.35	2.8	0.9	0.8	37.646
GaAs	1.52	5.8	1.3	−0.6	40.634
GaSb	0.81	3.0	−1.0	0.7	52.488
AlP	2.50	2.5	−1.0	0.4	40.637
AlAs	2.23	4.8	0.2	−1.1	43.616
AlSb	1.69	2.3	−3.8	0.7	56.607
InP	1.42	2.7	0.7	0.1	46.040
InAs	0.42	4.9	3.0	−1.5	49.123
InSb	0.24	2.2	0.5	0.1	62.908
MAE		3.24	1.27	0.63	
Metals					
Al-sc	0	0.32	0.32	−0.52	19.937
Al-fcc	0	1.95	1.95	2.44	16.575
Al-bcc	0	0.97	0.97	1.94	17.025
Mg-sc	0	0.62	0.62	1.07	27.107
Mg-fcc	0	1.28	1.28	1.28	23.073
Mg-bcc	0	1.42	1.42	1.25	22.939
Li-sc	0	0.20	0.20	0.46	19.932
Li-fcc	0	0.22	0.22	0.52	19.308
Li-bcc	0	0.22	0.22	0.51	19.397
MAE		0.80	0.80	1.11	

TABLE II. Errors of OF-DFT with respect to the KS-DFT references (OFDFT–KSDFT) for bulk moduli (GPa), computed from different KE functionals. The KS reference values (from Refs. [66,87]) are reported in the last column, and the exact band-gap energies (in eV) used for the KGAP functional are shown in the second column. The last lines of every panel report the mean absolute errors (MAE).

	E_g (eV)	SM	KGAP	HC	KS
Semiconductors					
Si	1.17	−42	−14.2	0.9	98
GaP	2.35	−28	−2.8	−14	80
GaAs	1.52	−35	−12.8	−3	75
GaSb	0.81	−21	−6.4	−6	56
AlP	2.50	−32	−8.6	1	90
AlAs	2.23	−33	−10.8	4	80
AlSb	1.69	−23	2.3	−1	60
InP	1.42	−25	−14.1	5	73
InAs	0.42	−24	−17.7	4	65
InSb	0.24	−17	−13.1	1	50
MAE		27.91	10.28	4.00	
Metals					
Al-sc	0	4.1	4.1	1.8	57
Al-fcc	0	−13.8	−13.8	−28.0	77
Al-bcc	0	−5.3	−5.3	−24.4	70
Mg-sc	0	1.5	1.5	3.7	24
Mg-fcc	0	−0.3	−0.3	−3.2	38
Mg-bcc	0	1.2	1.2	−4.3	38
Li-sc	0	−0.1	−0.1	−0.6	17
Li-fcc	0	0.2	0.2	−0.2	17
Li-bcc	0	−0.5	−0.5	−0.9	16
MAE		3.00	3.00	7.64	

In Tables I and II, we report the results for equilibrium volumes and bulk moduli of semiconductors and simple metals. The mean absolute relative errors (MARE) and the standard deviations (StdDev) are illustrated in Fig. 4.

As shown in Fig. 3, among the nonlocal KE functionals with a density-independent kernel constructed from the LR of
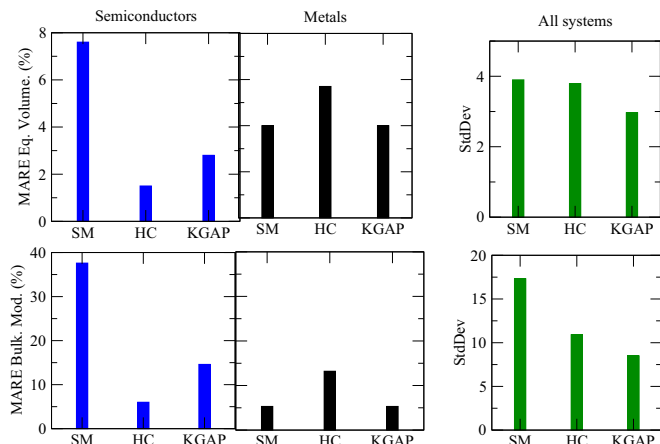

FIG. 4. Error statistics [mean absolute relative error (MARE) and standard deviation (StdDev)] of the OF-DFT calculations performed with SM [101], HC [85], and KGAP KE functionals. Full results are reported in Tables I and II.

the uniform electron gas, only the SM functional [101] shows converged results for semiconductors and a meaningful energy versus volume convex curve: for this reason, this is the only one reported in this section. Anyway, the performance of the SM functional is quite modest for semiconductors, giving a MARE of 7.5% for equilibrium volumes and a MARE of 38.1% for bulk moduli. On the other hand, accurate results are obtained for metals with a MARE of 4.0% for equilibrium volumes and MARE of 5.3% for bulk moduli. Nevertheless, we recall that the WGC and WT KE functionals are in general better than the SM functional, for simple metals [120].

An opposite trend is obtained for the HC functional which has been developed for semiconductors [85]. The MAREs for equilibrium volumes and bulk moduli are 1.4% and 6% for semiconductors, whereas much bigger errors are found for metals (5.7% and 13.2%, respectively). Thus, although the HC is very accurate for semiconductors, it is worse than SM for metals (improvement can be obtained employing dedicated fitting parameters).

The KGAP functional is significantly better than the SM functional for semiconductors. For equilibrium volumes, the MARE is 2.7% and for bulk moduli the MARE is below 14.6%, thus not far from the HC. By construction, the KGAP functional is equivalent to SM for metals, so that KGAP is reasonably accurate for these systems. Note that for bulk moduli the mean absolute error is about 10 GPa, being comparable or even smaller than that due to the use of XC

approximations in full KS-DFT calculations (see, for example, Table I of Ref. [121]).

In the right panels of Fig. 4, we report the standard deviations considering both semiconductors and metals, in order to measure if a given functional describes different systems with similar accuracy. The SM functional describes very differently metals and semiconductors, so the StdDev is large, in particular for the bulk modulus (StdDev = 17%). The HC functional has similar StdDev as SM functional for the equilibrium volume, whereas it is smaller for the bulk modulus (StdDev = 11%). On the other hand, the KGAP functional gives significantly reduced StdDev for both properties.

V. CONCLUSIONS

We have constructed a simple nonlocal KE functional named KGAP, with a density-independent kernel found from the linear response of the jellium-with-gap model. This functional has the correct physics of metals, semiconductors, and insulators in the $\mathbf{q} \to 0$ limit, being also very accurate for small perturbations of the density with large wave vectors. The KGAP functional performs well in the orbital-free DFT context, converging very fast and being equally accurate for metals (where by construction recovers the SM functional), and semiconductors. To our knowledge, the KGAP functional is the only one from the class of approximations with density-independent kernels, that has a rather broad applicability in solid-state physics.

In this first implementation, the KGAP functional has been tested on simple bulk systems. In this case, the KGAP semiempirical functional requires the *a priori* knowledge of the E_g parameter which can be well approximated by the fundamental band-gap energy of the system. For more general applications (e.g., interfaces), the E_g parameter must be spatially dependent, as shown for example in Refs. [61,115,122]. Such a KE functional will be more complicated than the simple KGAP, but we expect it to be very accurate. We will address this important issue in next work.

APPENDIX A

Let consider a functional $J[n]$ of the form

$$J[n] = \int \int d\mathbf{r}\, d\mathbf{r}'\, n^\alpha(\mathbf{r}) w(\mathbf{r} - \mathbf{r}') n^\beta(\mathbf{r}'), \quad \text{(A1)}$$

with α and β positive constants. Using the definition of functional derivative

$$\int \frac{\delta J}{\delta n(\mathbf{r})} \phi(\mathbf{r}) d\mathbf{r} = \frac{d}{d\epsilon} J[n + \epsilon\phi]\,|_{\epsilon=0}, \quad \text{(A2)}$$

we find

$$\frac{\delta J}{\delta n(\mathbf{r})} = \int d\mathbf{r}'\, w(\mathbf{r} - \mathbf{r}')\{\alpha n(\mathbf{r})^{\alpha-1} n(\mathbf{r}')^\beta + \beta n(\mathbf{r}')^\alpha n(\mathbf{r})^{\beta-1}\}.$$
$$\text{(A3)}$$

Finally, we obtain

$$\left.\frac{\delta^2 J}{\delta n(\mathbf{r})\delta n(\mathbf{r}')}\right|_{n=n_0} = 2\alpha\beta n_0^{\alpha+\beta-2} w(\mathbf{r} - \mathbf{r}'). \quad \text{(A4)}$$

Equation (A4) combined with Eqs. (7) and (8) give Eq. (10).

APPENDIX B

For a given Δ, a series expansion of F^{GAP} for $\eta \to 0$ gives

$$F^{\mathrm{GAP}} \longrightarrow \frac{3\Delta^2}{16\eta^2} + \frac{9}{5} + \frac{3}{175}\frac{175\Delta^2 - 192}{\Delta^2}\eta^2 + \cdots. \quad \text{(B1)}$$

Thus, for any system with $\Delta > 0$ we have that $F^{\mathrm{GAP}} \propto \Delta^2\eta^{-2}$, which is the most relevant physical result. We recall that for semiconductors and insulators, the density response function behaves as [85,123]

$$-\frac{1}{\chi^{\mathrm{semicond}}(k)} \xrightarrow{k\to 0} \frac{b}{k^2}, \quad \text{(B2)}$$

with $b \geqslant 0$ being material dependent. Note that in the jellium-with-gap model, b is a function of the band gap E_g.

On the other hand, if we first perform a series expansion for $\Delta \to 0$, and then a series expansion for $\eta \to 0$ we obtain

$$F^{\mathrm{GAP}} \longrightarrow \left[1 + \frac{1}{3}\eta^2 + \frac{8}{45}\eta^4 + \cdots\right]$$
$$+ \Delta\left[\frac{\pi}{8}\frac{1}{\eta} + \frac{\pi}{12}\eta + \cdots\right] + \cdots,$$
$$F^{\mathrm{GAP}} = F^{\mathrm{Lind}}, \quad \text{when} \quad \Delta = 0 \quad \text{(B3)}$$

such that at small band gaps, F^{GAP} is close to the Lindhard function F^{Lind}:

$$F^{\mathrm{GAP}} \to F^{\mathrm{Lind}} + O(\Delta) + \cdots \text{ for } \Delta \to 0. \quad \text{(B4)}$$

In the limit of large wave vectors, i.e., for $\eta \to \infty$, we have

$$F^{\mathrm{GAP}} \to 3\eta^2 - \frac{3}{5} + \left(-\frac{24}{175} + \frac{3}{16}\Delta^2\right)\frac{1}{\eta^2} + O\left(\frac{1}{\eta^4}\right). \quad \text{(B5)}$$

Therefore, in this limit, F^{GAP} always behaves as F^{Lind} for $\Delta = 0$. Moreover, for any Δ and η, the following inequality holds (see Fig. 2 of Ref. [61]):

$$F^{\mathrm{GAP}} \geqslant F^{\mathrm{Lind}}. \quad \text{(B6)}$$

APPENDIX C

Following Ref. [86], we can write Eq. (7) in momentum space as

$$T_s[n] = \Omega \sum_{\mathbf{q}} \tilde{t}_s^{\alpha,\beta}(\mathbf{q}),$$

$$\tilde{t}_s^{\alpha,\beta}(\mathbf{q}) = \lambda\tilde{t}_{\mathrm{TF}}(\mathbf{q}) + \mu\tilde{t}_W(\mathbf{q}) + \tilde{t}_X^{\alpha,\beta}(\mathbf{q}),$$

$$\tilde{t}_{\mathrm{TF}}(\mathbf{q}) = \frac{3}{10}(3\pi^2)^{2/3} n_{\mathbf{q}}^{5/6} n_{-\mathbf{q}}^{5/6},$$

$$\tilde{t}_W(\mathbf{q}) = \frac{1}{2} n_{\mathbf{q}}^{1/2} q^2 n_{-\mathbf{q}}^{1/2}. \quad \text{(C1)}$$

Let us consider the partition (see also Ref. [86])

$$\tilde{t}_X^{\alpha,\beta}(\mathbf{q}) = -t_{\mathrm{I}}(\mathbf{q}) - t_{\mathrm{II}}(\mathbf{q}) - t_{\mathrm{III}}(\mathbf{q}), \quad \text{(C2)}$$

where

$$t_{\mathrm{I}}(\mathbf{q}) = \frac{1}{2\alpha\beta n_0^{\alpha+\beta-2}} n_{\mathbf{q}}^{\alpha} \frac{1}{\chi^{\mathrm{GAP}}} n_{-\mathbf{q}}^{\beta},$$

$$t_{\mathrm{II}}(\mathbf{q}) = \lambda \frac{k_F^2}{6\alpha\beta n_0^{\alpha+\beta-1}} n_{\mathbf{q}}^{\alpha} n_{-\mathbf{q}}^{\beta},$$

$$t_{\mathrm{III}}(\mathbf{q}) = \mu \frac{1}{8\alpha\beta n_0^{\alpha+\beta-1}} n_{\mathbf{q}}^{\alpha} q^2 n_{-\mathbf{q}}^{\beta}. \tag{C3}$$

Note that, for simplicity of notation, we use $n_{\mathbf{q}}^{\alpha} G n_{-\mathbf{q}}^{\beta}$ instead of the symmetric function $\frac{1}{2}\{n_{\mathbf{q}}^{\alpha} G n_{-\mathbf{q}}^{\beta} + n_{\mathbf{q}}^{\beta} G n_{-\mathbf{q}}^{\alpha}\}$.

From Appendix B, we find

$$\lim_{\mathbf{q}\to 0} \lim_{\Delta\to 0} \frac{1}{\chi^{\mathrm{GAP}}} = -\frac{1}{3n_0}\left(k_F^2 + \frac{q^2}{12}\right),$$

$$\lim_{\mathbf{q}\to\infty} \frac{1}{\chi^{\mathrm{GAP}}} = \frac{1}{n_0}\left(\frac{k_F^2}{5} - \frac{q^2}{4}\right), \tag{C4}$$

then, substituting Eq. (C4) into Eq. (C3), we find after some algebra

$$\lim_{\mathbf{q}\to 0} t_{\mathrm{I}}(\mathbf{q}) = -\frac{1}{\lambda} t_{\mathrm{II}}(\mathbf{q}) - \frac{1}{9\mu} t_{\mathrm{III}}(\mathbf{q}),$$

$$\lim_{\mathbf{q}\to 0} \tilde{t}_s(\mathbf{q}) = \lambda \tilde{t}_{\mathrm{TF}}(\mathbf{q}) + \mu \tilde{t}_W(\mathbf{q}) + t_{\mathrm{II}}(\mathbf{q})\left(\frac{1}{\lambda} - 1\right)$$

$$+ t_{\mathrm{III}}(\mathbf{q})\left(\frac{1}{9\mu} - 1\right),$$

$$\lim_{\mathbf{q}\to\infty} t_I(\mathbf{q}) = \frac{3}{5\lambda} t_{\mathrm{II}}(\mathbf{q}) - \frac{1}{\mu} t_{\mathrm{III}}(\mathbf{q}),$$

$$\lim_{\mathbf{q}\to\infty} \tilde{t}_s(\mathbf{q}) = \lambda \tilde{t}_{\mathrm{TF}}(\mathbf{q}) + \mu \tilde{t}_W(\mathbf{q}) - t_{\mathrm{II}}(\mathbf{q})\left(\frac{3}{5\lambda} + 1\right)$$

$$+ t_{\mathrm{III}}(\mathbf{q})\left(\frac{1}{\mu} - 1\right). \tag{C5}$$

Performing the integrals, we find

$$T_{\mathrm{III}}$$

$$= \Omega \sum_{\mathbf{q}} \mu \frac{1}{8\alpha\beta n_0^{\alpha+\beta-1}} n_{\mathbf{q}}^{\alpha} q^2 n_{-\mathbf{q}}^{\beta}$$

$$= \mu T_s^W + \mu(\alpha + \beta - 1)\left\{\langle \delta n|t_W\rangle + \frac{(\alpha+\beta-2)}{2}\langle \delta^2 n|t_W\rangle\right\} \tag{C6}$$

and

$$T_{\mathrm{II}} = \lambda \frac{5}{9\alpha\beta} T_s^{\mathrm{TF}} + \lambda \frac{5}{9\alpha\beta}\left(\alpha + \beta - \frac{5}{3}\right)$$

$$\times \left\{\langle \delta n|t_{\mathrm{TF}}\rangle + \frac{1}{2}\left(\alpha + \beta - \frac{8}{3}\right)\langle \delta^2 n|t_{\mathrm{TF}}\rangle\right\}. \tag{C7}$$

Combining Eqs. (C5)–(C7), we obtain Eqs. (11) and (12).

---

[1] P. Hohenberg and W. Kohn, Phys. Rev. **136**, B864 (1964).

[2] M. Levy, Proc. Natl. Acad. Sci. USA **76**, 6062 (1979).

[3] G. E. Scuseria and V. N. Staroverov, *Theory and Applications of Computational Chemistry* (Elsevier, 2005), pp. 669–724.

[4] F. Della Sala, E. Fabiano, and L. A. Constantin, Int. J. Quantum Chem. **116**, 1641 (2016).

[5] Y. A. Wang and E. A. Carter, *Theoretical Methods in Condensed Phase Chemistry* (Springer, Berlin, 2002), pp. 117–184.

[6] V. V. Karasiev, D. Chakraborty, and S. B. Trickey, *Many-Electron Approaches in Physics, Chemistry and Mathematics* (Springer, Switzerland, 2014), pp. 113–134.

[7] J. C. Snyder, M. Rupp, K. Hansen, K.-R. Müller, and K. Burke, Phys. Rev. Lett. **108**, 253002 (2012).

[8] K. Yao and J. Parkhill, J. Chem. Theory Comput. **12**, 1139 (2016).

[9] P. García-González, J. E. Alvarellos, and E. Chacón, Phys. Rev. A **54**, 1897 (1996).

[10] I. A. Howard, N. H. March, and V. E. Van Doren, Phys. Rev. A **63**, 062501 (2001).

[11] N. March and R. Santamaria, Int. J. Quantum Chem. **39**, 585 (1991).

[12] F. Della Sala, E. Fabiano, and L. A. Constantin, Phys. Rev. B **91**, 035126 (2015).

[13] W. Kohn and L. J. Sham, Phys. Rev. **140**, A1133 (1965).

[14] F. Tran, J. Stelzl, and P. Blaha, J. Chem. Phys. **144**, 204120 (2016).

[15] K. Burke, J. Chem. Phys. **136**, 150901 (2012).

[16] S. Goedecker, Rev. Mod. Phys. **71**, 1085 (1999).

[17] S. Goedecker and G. E. Scuseria, Comput. Sci. Eng. **5**, 14 (2003).

[18] P. Vogl, H. P. Hjalmarson, and J. D. Dow, J. Phys. Chem. Solids **44**, 365 (1983).

[19] J. N. Murrell, J. Mol. Struct.: THEOCHEM **424**, 93 (1998).

[20] M. Wahiduzzaman, A. F. Oliveira, P. Philipsen, L. Zhechkov, E. van Lenthe, H. A. Witek, and T. Heine, J. Chem. Theory Comput. **9**, 4006 (2013).

[21] L. Hung and E. A. Carter, Chem. Phys. Lett. **475**, 163 (2009).

[22] F. Lambert, J. Clérouin, and S. Mazevet, Europhys. Lett. **75**, 681 (2006).

[23] M. Chen, L. Hung, C. Huang, J. Xia, and E. A. Carter, Mol. Phys. **111**, 3448 (2013).

[24] V. Gavini, K. Bhattacharya, and M. Ortiz, J. Mech. Phys. Solids **55**, 697 (2007).

[25] B. Radhakrishnan and V. Gavini, Phys. Rev. B **82**, 094117 (2010).

[26] V. Gavini, Phys. Rev. Lett. **101**, 205503 (2008).

[27] B. Radhakrishnan and V. Gavini, Philos. Mag. **96**, 2468 (2016).

[28] K. J. Caspersen and E. A. Carter, Proc. Natl. Acad. Sci. USA **102**, 6738 (2005).

[29] H. Xiang, M. Zhang, X. Zhang, and G. Lu, J. Phys. Chem. C **120**, 14330 (2016).

[30] P. W. Ayers, R. G. Parr, and A. Nagy, Int. J. Quantum Chem. **90**, 309 (2002).

[31] J. S. Anderson, P. W. Ayers, and J. I. R. Hernandez, J. Phys. Chem. A **114**, 8884 (2010).

[32] L. H. Thomas, in *Mathematical Proceedings of the Cambridge Philosophical Society*, Vol. 23 (Cambridge University Press, Cambridge, 1927), pp. 542–548.

[33] E. Fermi, Rend. Accad. Naz. Lincei **6**, 32 (1927).

[34] E. H. Lieb and B. Simon, Phys. Rev. Lett. **31**, 681 (1973).

[35] E. Teller, Rev. Mod. Phys. **34**, 627 (1962).

[36] E. H. Lieb, Rev. Mod. Phys. **48**, 553 (1976).

[37] E. H. Lieb, Rev. Mod. Phys. **53**, 603 (1981).

[38] E. H. Lieb and B. Simon, Adv. Math. **23**, 22 (1977).

[39] O. J. Heilmann and E. H. Lieb, Phys. Rev. A **52**, 3628 (1995).

[40] L. A. Constantin, J. C. Snyder, J. P. Perdew, and K. Burke, J. Chem. Phys. **133**, 241103 (2011).

[41] C. F. von Weizsäcker, Z. Phys. A **96**, 431 (1935).

[42] R. Benguria, H. Brézis, and E. H. Lieb, Commun. Math. Phys. **79**, 167 (1981).

[43] M. Levy and Hui Ou-Yang, Phys. Rev. A **38**, 625 (1988).

[44] C. Herring, Phys. Rev. A **34**, 2614 (1986).

[45] M. Levy and J. P. Perdew, Phys. Rev. A **32**, 2010 (1985).

[46] E. Fabiano and L. A. Constantin, Phys. Rev. A **87**, 012511 (2013).

[47] P. W. Ayers, J. Math. Phys. **46**, 062107 (2005).

[48] M. Levy and P. Ziesche, J. Chem. Phys. **115**, 9110 (2001).

[49] A. Nagy and N. March, Phys. Chem. Liquids **25**, 37 (1992).

[50] A. Nagy, Int. J. Quantum Chem. **110**, 2117 (2010).

[51] A. Nagy, Int. J. Quantum Chem. **115**, 1392 (2015).

[52] D. Kirzhnitz, Exptl. Theoret. Phys. (U.S.S.R.) **32**, 115 (1957) [Sov. Phys.–JETP **5**, 64 (1957)].

[53] L. A. Constantin, E. Fabiano, S. Laricchia, and F. Della Sala, Phys. Rev. Lett. **106**, 186406 (2011).

[54] S. Laricchia, E. Fabiano, L. Constantin, and F. Della Sala, J. Chem. Theory Comput. **7**, 2439 (2011).

[55] H. Ou-Yang and M. Levy, Int. J. Quantum Chem. **40**, 379 (1991).

[56] J. P. Perdew, Phys. Lett. A **165**, 79 (1992).

[57] M. Ernzerhof, J. Mol. Struct.: THEOCHEM **501-502**, 59 (2000).

[58] L. A. Constantin and A. Ruzsinszky, Phys. Rev. B **79**, 115117 (2009).

[59] L. Vitos, B. Johansson, J. Kollar, and H. L. Skriver, Phys. Rev. A **61**, 052511 (2000).

[60] A. Lindmaa, A. E. Mattsson, and R. Armiento, Phys. Rev. B **90**, 075139 (2014).

[61] L. A. Constantin, E. Fabiano, S. Śmiga, and F. Della Sala, Phys. Rev. B **95**, 115153 (2017).

[62] A. Borgoo and D. J. Tozer, J. Chem. Theory Comput. **9**, 2250 (2013).

[63] A. J. Thakkar, Phys. Rev. A **46**, 6920 (1992).

[64] A. Lembarki and H. Chermette, Phys. Rev. A **50**, 5328 (1994).

[65] J. Seino, R. Kageyama, M. Fujinami, Y. Ikabata, and H. Nakai, J. Chem. Phys. **148**, 241705 (2018).

[66] J. Xia and E. A. Carter, Phys. Rev. B **91**, 045124 (2015).

[67] S. B. Trickey, V. V. Karasiev, and D. Chakraborty, Phys. Rev. B **92**, 117101 (2015).

[68] J. Xia and E. A. Carter, Phys. Rev. B **92**, 117102 (2015).

[69] V. V. Karasiev, T. Sjostrom, and S. B. Trickey, Comput. Phys. Commun. **185**, 3240 (2014).

[70] V. V. Karasiev and S. B. Trickey, Adv. Quantum Chem. **71**, 221 (2015).

[71] V. V. Karasiev, S. B. Trickey, and F. E. Harris, J. Comput.-Aided Mater. Des. **13**, 111 (2006).

[72] V. V. Karasiev, D. Chakraborty, O. A. Shukruto, and S. B. Trickey, Phys. Rev. B **88**, 161108 (2013).

[73] M. Brack, B. K. Jennings, and Y. H. Chu, Phys. Lett. B **65**, 1 (1976).

[74] C. H. Hodges, Can. J. Phys. **51**, 1428 (1973).

[75] E. Engel and J. P. Perdew, Phys. Rev. B **43**, 1331 (1991).

[76] E. Engel, P. LaRocca, and R. M. Dreizler, Phys. Rev. B **49**, 16728 (1994).

[77] A. C. Cancio, D. Stewart, and A. Kuna, J. Chem. Phys. **144**, 084107 (2016).

[78] A. C. Cancio and J. J. Redd, Mol. Phys. **115**, 618 (2017).

[79] S. Laricchia, L. A. Constantin, E. Fabiano, and F. Della Sala, J. Chem. Theory Comput. **10**, 164 (2013).

[80] L. A. Constantin, E. Fabiano, and F. Della Sala, arXiv:1802.02889v2.

[81] L. A. Constantin, E. Fabiano, and F. Della Sala, J. Chem. Phys. **145**, 084110 (2016).

[82] L. A. Constantin, E. Fabiano, and F. Della Sala, J. Chem. Theory Comput. **13**, 4228 (2017).

[83] E. Prodan and W. Kohn, Proc. Natl. Acad. Sci. USA **102**, 11635 (2005).

[84] L. A. Constantin, E. Fabiano, and F. Della Sala, Computation **4**, 19 (2016).

[85] C. Huang and E. A. Carter, Phys. Rev. B **81**, 045206 (2010).

[86] Y. A. Wang, N. Govind, and E. A. Carter, Phys. Rev. B **58**, 13465 (1998).

[87] I. Shin and E. A. Carter, J. Chem. Phys. **140**, 18A531 (2014).

[88] G. S. Ho, V. L. Lignères, and E. A. Carter, Phys. Rev. B **78**, 045105 (2008).

[89] J. A. Alonso and L. A. Girifalco, Phys. Rev. B **17**, 3735 (1978).

[90] P. García-González, J. E. Alvarellos, and E. Chacón, Phys. Rev. B **53**, 9509 (1996).

[91] E. Chacón, J. E. Alvarellos, and P. Tarazona, Phys. Rev. B **32**, 7868 (1985).

[92] P. García-González, J. E. Alvarellos, and E. Chacón, Phys. Rev. B **57**, 4857 (1998).

[93] D. Garcia-Aldea and J. E. Alvarellos, Phys. Rev. A **77**, 022502 (2008).

[94] W. Mi, A. Genova, and M. Pavanello, J. Chem. Phys. **148**, 184107 (2018).

[95] E. V. Ludeña, E. X. Salazar, M. H. Cornejo, D. E. Arroyo, and V. V. Karasiev, Int. J. Quantum Chem. (2018), DOI:10.1002/qua.25601.

[96] E. X. Salazar, P. F. Guarderas, E. V. Ludena, M. H. Cornejo, and V. V. Karasiev, Int. J. Quantum Chem. **116**, 1313 (2016).

[97] Y. A. Wang, N. Govind, and E. A. Carter, Phys. Rev. B **60**, 16350 (1999).

[98] J. Lindhard, Kgl. Danske Videnskab. Selskab Mat.-Fys. Medd. **28**, 1 (1954).

[99] F. Perrot, J. Phys.: Condens. Matter **6**, 431 (1994).

[100] L.-W. Wang and M. P. Teter, Phys. Rev. B **45**, 13196 (1992).

[101] E. Smargiassi and P. A. Madden, Phys. Rev. B **49**, 5220 (1994).

[102] J. Xia and E. A. Carter, Phys. Rev. B **86**, 235109 (2012).

[103] I. Shin, Mechanical properties of lightweight metals from first principles orbital-free density functional theory, Ph.D. thesis, Princeton University, 2013.

[104] Z. H. Levine and S. G. Louie, Phys. Rev. B **25**, 6310 (1982).

[105] J. Callaway, Phys. Rev. **116**, 1368 (1959).

[106] D. R. Penn, Phys. Rev. **128**, 2093 (1962).

[107] G. Srinivasan, Phys. Rev. **178**, 1244 (1969).

[108] A. Tsolakidis, E. L. Shirley, and R. M. Martin, Phys. Rev. B **69**, 035104 (2004).

[109] P. E. Trevisanutto, A. Terentjevs, L. A. Constantin, V. Olevano, and F. Della Sala, Phys. Rev. B **87**, 205143 (2013).

[110] J. Rey and A. Savin, Int. J. Quantum Chem. **69**, 581 (1998).

[111] J. Krieger, J. Chen, G. Iafrate, A. Savin, A. Gonis, and N. Kioussis, *Electron Correlations and Materials Properties* (Springer, New York, 1999), pp. 463–477

[112] J. Krieger, J. Chen, and S. Kurth, *Density Functional Theory and its Application to Materials,* AIP Conference Proceedings, Vol. 577 (AIP, New York, 2001), pp. 48–69.

[113] J. Toulouse, A. Savin, and C. Adamo, J. Chem. Phys. **117**, 10465 (2002).

[114] J. Toulouse and C. Adamo, Chem. Phys. Lett. **362**, 72 (2002).

[115] E. Fabiano, P. E. Trevisanutto, A. Terentjevs, and L. A. Constantin, J. Chem. Theory. Comput. **10**, 2016 (2014).

[116] G. S. Ho, V. L. Lignères, and E. A. Carter, Comput. Phys. Commun. **179**, 839 (2008).

[117] J. P. Perdew and A. Zunger, Phys. Rev. B **23**, 5048 (1981).

[118] J. P. Perdew, K. Burke and M. Ernzerhof, Phys. Rev. Lett. **77**, 3865 (1996).

[119] F. Murnaghan, Proc. Natl. Acad. Sci. U. S. A. **30**, 244 (1944).

[120] K. M. Carling and E. A. Carter, Modell. Simul. Mater. Sci. Eng. **11**, 339 (2003).

[121] L. A. Constantin, A. Terentjevs, F. Della Sala, P. Cortona, and E. Fabiano, Phys. Rev. B **93**, 045126 (2016).

[122] A. Terentjevs, P. E. Trevisanutto, L. A. Constantin, and F. Della Sala, J. Phys.: Condens. Matter **26**, 265006 (2014).

[123] R. M. Pick, M. H. Cohen, and R. M. Martin, Phys. Rev. B **1**, 910 (1970).